steel research international
www.steel-research.de

Effect of the Al_2O_3 Content in the Slag on the Remelting Behavior of a Bearing Steel

Reinhold S. E. Schneider, Manuel Molnar, Gerald Klösch, Christopher Schüller, and Josef Fasching*

The service life of roller bearings strongly depends on nonmetallic inclusions (NMIs). Therefore, these steels request highest metallurgical standards in their production. To determine the effect of the Al_2O_3 content and a protective atmosphere (N_2) on the electroslag remelting (ESR) behavior, laboratory scale experiments are conducted. Changes in the composition of the remelted materials and in the slag are determined. In addition, the amount and composition of the NMI prior and after remelting are investigated, and thermodynamic simulations on the formation of NMI are conducted. Changes in the chemical composition can largely be explained by well-known equilibrium reactions between the slag and the metal. Lowest Al contents in the remelted steel can only be achieved with the Al_2O_3-free slag. Higher Al_2O_3 contents in the slag lead to higher oxygen and sulfur contents in the steel and corresponding higher amounts of NMI after remelting. The use of a protective gas mainly reduced the loss of Si and led to lower O and S contents after remelting with the Al_2O_3-free slag. The composition of the NMI changed from alumina type to $MgO–Al_2O_3$ (MA)-spinel type and finally mixed $MgO–SiO_2$ oxides with decreasing Al_2O_3 contents. These results are confirmed by thermodynamic calculations.

1. Introduction

Bearing steels can be exposed to extreme service environments such as high contact pressure, high rotational speed, and/or elevated temperatures. Rolling contact fatigue (RCF) is therefore a key factor affecting the bearings life. Many authors in previous studies[1–11] have pointed out that nonmetallic inclusions (NMIs), in addition to other factors such as hardness, toughness, and residual stresses, have a significant influence on these fatigue properties. The maximum inclusion size is considered to be the most relevant factor.[1–7] $SiO_2–Al_2O_3$ inclusions are regarded less harmful than Al_2O_3 or $Al_2O_3–CaO$ inclusions and the sulfur content, resulting in different amounts of sulfides, has also a strong effect on RCF.[1,11] Microcracks are preferentially initiated at complex oxisulfides rather than plain sulfides, but no simple relationships can be established.[8] Compared with many other steel grades, NMI in bearing steels occur typically in low or very low volume fractions.[1–5,9] However, at oxygen contents below 10 ppm, the particle size distribution of oxide inclusions can differ quite significantly at almost same oxygen contents.[4] Recent investigations on super clean bearing steels have shown, that MnS-type inclusions are not that harmful, whereas Al_2O_3, TiN as well as silicates act as favorable sites for crack nucleation.[3] According to the study by Ebert,[9] the elastic properties, hardness, and brittleness of NMI play a decisive role. The NMI size distribution, orientation as well as the hot forming process can also influence RCF conditions[7,8] but published works on the effect of hot deformation is still sparse.[5] The inclusion–matrix interface, in correlation with the chemical composition of the NMI, plays also an important role for RCF,[2,3,5,9–11] thereby hot isostatic pressing (HIP) can increase RCF life by closing cavities between inclusions and metal matrix.[10] As a consequence, the production of high-purity bearing steels is still one of the most demanding challenges in steel metallurgy.

Electroslag remelting was developed and is still mainly used to reduce inhomogeneity such as segregations and shrink holes and to improve the cleanliness level, especially regarding large NMI.[12–16] The cleanliness level and the type of inclusions depend significantly on the remelting slag.[12,13,17–21] The composition and basicity of the slag also have a major effect on silicon losses.[12,13,20,22] However, detailed investigations on the effect of various slag compositions on the formation and composition of NMI during remelting are still limited, but this topic has gained recent interest to produce steels with lowest amounts of oxygen and NMI.

Prof. R. S. E. Schneider, M. Molnar
School of Engineering
University of Applied Sciences Upper Austria – Research and Development
Roseggerstraße 15, 4600 Wels, Austria
E-mail: r.schneider@fh-wels.at

M. Molnar
K1-MET GmbH
Stahlstraße 14, 4020 Linz, Austria

Dr. G. Klösch, C. Schüller, Dr. J. Fasching
voestalpine Stahl Donawitz GmbH
Kerpelystrasse 199, 8700 Leoben, Austria

The ORCID identification number(s) for the author(s) of this article can be found under https://doi.org/10.1002/srin.202000241.

DOI: 10.1002/srin.202000241

Laboratory experiments starting from a higher oxygen content in the electrode and using a protective atmosphere as well as additions of deoxidants to the slag on a corrosion resistant die steel is described in the study by Shi et al.,[16] showing a significant reduction of the inclusion content. The effects of a protective atmosphere and different slag compositions on the remelting behavior of a hot work tool steel can be found in the study by Schneider et al.[23] The protective gas eliminated the scaling of the electrode and corresponding silicon losses but had little effects on NMI, which were dominantly $MgO–Al_2O_3$ (MA)-spinel. In contrast, using a CaO-free slag had the strongest effect on the steel composition and shifted the NMI composition toward aluminates. Other laboratory-scale investigations on a die steel show advantages of a protective gas, low filling rations, and a multicomponent slag over a binary $CaF_2–Al_2O_3$–slag.[24] The majority of the inclusions were MA-spinel or Al_2O_3 type, but more detailed information are missing for better comparison.

The origin of NMI in a steel produced under industrial conditions indicate, that many NMI are formed newly during solidification, whereas some especially MgO and MA-spinel-type inclusions originate from the electrode.[25,26] Results from industrial production in the study by Mitchell[15] confirm the strong cleaning effect of electroslag remelting (ESR) almost similar to vacuum arc remelting, especially when using a protective atmosphere. Most of the detected NMI from industrial ESR of hot work tool steels were of the MA-spinel type or have a high Al_2O_3 content.[27,28]

The effect of higher SiO_2 contents in the remelting slag on the NMI composition of a hot work tool steel in the studies by Schneider et al.[23,29] confirms earlier results in the studies by Holzgruber and Plöckinger and Allibert et al.[12,20] that larger inclusions with high SiO_2 contents are formed. Experiments with a similar steel grade, but a higher oxygen content, confirmed MA-spinel as dominating type of inclusions, but no effect of the SiO_2 content in the slag on the SiO_2 content in the inclusions after remelting could be found.[30] These results were confirmed by thermodynamic calculations. Using higher MgO contents in the remelting slag lead to a reduction of larger NMI in a creep-resistant steel.[10] However, the number of inclusions less than 4 μm increased with raising magnesia content.

Results in the study by Li et al.[31] indicate that slags with 20–25% SiO_2, with or without Al_2O_3, can be used to produce bearing steels with mullite-type inclusions. The remelting of roller bearing steels as described in the study by Randak et al.,[32] showed significant advantages, especially in the amount of NMI. However, modern conventional steelmaking praxis results in excellent microstructures, reduced segregations, and low amounts of NMIs.[33] Nevertheless, further improvements to remove larger NMI or to change their chemical composition seem feasible by ESR.

In this work, the effects of three different Al_2O_3 contents (0, 6% and 33%) during remelting of a roller bearing steel were investigated. Thereby, the changes in the chemical composition, especially aluminum, silicon, magnesium, oxygen, and sulfur as well as corresponding changes in type, content, and composition of the NMI were investigated and thermodynamically simulated. Additional results on the size distribution of the NMI can be found in the study by Schneider et al.[34]

2. Experimental Section

All experiments described in this article were conducted on a laboratory-scale ESR plant. Information on the plant configuration can be found in the study by Schneider et al.[35]

2.1. Investigated Materials

The continuous cast and rolled ball bearing steel 100Cr6 (mat. no. 1.3505, ASTM 52100) was used. The chemical composition of the steel is shown in **Table 1**. All electrodes had a diameter of 70 mm and a bright machined surface. Three different slags with Al_2O_3 contents of 0, 6, and 33 wt%, were investigated. One slag (A33) was a standard ESR slag containing roughly 1/3 CaF_2, CaO, and Al_2O_3 each as well as smaller amounts ($\leq$3%) of SiO_2 and MgO. The other slags (A6 and A0) were also CaF_2–CaO-based and contained $\approx$7% SiO_2, 4% MgO, and 6%, respectively, 0% Al_2O_3.

2.2. Process Parameters

All experiments were operated with a frequency of 4.5 Hz in a mold with 125 mm diameter. Starting was conducted with solid slag and 3 g of Al-granulate for initial deoxidation. For this "cold start procedure," the electrode was contacted with the Al-granulate and the baseplate, forming an open arc. Subsequently granulated solid slag components were added into the mold. The arc does not only melt the electrode but also the solid slag, thereby changing the system from initial arc heating to resistance heating. The whole slag is typically completely melted after 10–15 min. The other operating parameters, especially the melting current, were selected to realize comparable melt rates of about 30 kg h^{-1}, thereby only trial A6 showed a significantly higher value (**Table 2**). The voltage is the result of the amount of slag, the immersion depth (0.5–1 cm) and the electrical conductivity of the slag. Three remelting trials were conducted using a protective gas atmosphere with nitrogen (the oxygen content was measured and controlled to be $\leq$0.1 vol%). The other three ingots were remelted in open operation and contact to air. No deoxidants were added during the remelting. The ingot length after remelting was between 500 and 530 mm.

Table 1. Chemical compositions of the electrode and the remelted ingots.

Trial, slag	C [wt%]	Si [wt%]	Mn [wt%]	Cr [wt%]	Al [wt%]	S [ppm]	O [ppm]	N [ppm]	Mg [ppm]
Electrode	1.04	0.294	0.295	1.506	0.0012	107	8	47	–*[a)]
A33	1.04	0.202	0.293	1.500	0.0163	23	63	44	–*[a)]
A33-N	1.03	0.254	0.281	1.500	0.0459	53	70	57	1
A6	1.01	0.137	0.294	1.505	0.0025	22	62	35	–*[a)]
A6-N	1.04	0.268	0.284	1.501	0.0125	24	66	96	10
A0	1.01	0.144	0.294	1.495	0.0007	23	63	31	–*[a)]
A0-N	1.03	0.276	0.288	1.506	0.0008	4	21	106	12

[a)]–* ... below detection limit of 1 ppm.

Table 2. Process parameters of the remelting experiments.

Trial, slag	[Atmosphere]	Al_2O_3 [wt%]	SiO_2 [wt%]	MgO [wt%]	Slag [kg]	Current [kA]	Voltage [V]	Melt rate [$kg\,h^{-1}$]
A33	Air	33	1.5	3	2.0	2.4	≈61	29
A33-N	N_2	33	1.5	3	2.0	2.4	≈62	27
A6	Air	6	7.5	4	2.6	3.4	≈62	38
A6-N	N_2	6	7.5	4	2.6	3.4	≈62	28
A0	Air	0	7.5	4	2.6	3.1	≈54	33
A0-N	N_2	0	7.5	4	2.6	3.6	≈59	29

2.3. Materials Investigation

The remelted ingots were forged to a final diameter of 40 mm. The forging operation started at a temperature of 1200 °C and was conducted in one heat. The degree of deformation $A_{\mathrm{initial}}/A_{\mathrm{end}}$ was roughly 10. Samples were taken from the upper third of the forged ingot for chemical analysis and investigations concerning NMIs were conducted. In addition, the top slag was analyzed after remelting, using pyrohydrolysis (Thermofischer AQF-2100H) for fluorine and X-ray fluorescence spectroscopy (Panalytical CubiX) for the other documented elements. Chemical analysis of the ingot was conducted by carrier gas hot extraction for C, S, O, and N (Leco CS 734 and Leco ON 736) and optical emission spectroscopy (OES) (Thermo ARL 4460) for all other elements. A scanning electron microscope (SEM) (Zeiss GeminiSEM) fitted with an Oxford Instruments X-Max X-ray energy dispersive detector (EDS) and the INCA software was used for the automated analysis of the NMIs. The system was equipped with a W emitter, and the analyses were carried out at an electron beam energy of 15 keV.

Automated NMI scans were conducted in the backscattered electron mode from standardized fields of 150 mm^2. Due to the lower atomic number of NMI typical elements such as O and S, NMI appeared darker than the surrounding metal matrix in this imaging mode, can therefore be detected easily and were subsequently analyzed by EDS. Thus, it was possible to fully characterize the position, size, and composition of all inclusions. A detailed description of this method, its advantages and limits can be found in the study by Werl et al.[36] NMI with an oxygen content of ≥5 wt% and an S:O-ratio lower than 0.15 were considered oxides. Inclusions containing more than 2 wt% oxygen and 1 wt% sulfur and an S:O ratio between 0.15 and 6.67 were categorized as oxisulfides. These type of NMI were usually conglomerates of oxides and sulfides. All detected NMI with a sulfur content of ≥2 wt% and an O:S ratio below 0.15 were taken as sulfides.

Thermodynamic calculations were carried out based on the chemical composition of the ingots, using "FactSage 7.3" in "Eqilib" mode. All solutions and pure solids, within the databases FactPS, FToxid, and FSsteel were considered as possible phases. Pure liquid and gas phases were excluded. The equilibrium was calculated in 5 K steps between 2200 and 1200 K as well as for all transition temperatures.

3. Results

3.1. Chemical Composition of the Ingots

The chemical composition of the remelted ingots in comparison with the electrode is shown in Table 2. There were no significant changes in the contents of C, Mn, and Cr due to the remelting process. Obviously, there is a rising N content after remelting with the N_2-protective atmosphere, which is strongest pronounced at the lowest Al_2O_3 content in the slag. In reverse, the N-content was slightly reduced after open remelting.

The changes of the elements Si, Al, O, and S are shown in **Figure 1**. Compared with the electrode, a slight reduction of the silicon content when remelting under nitrogen takes place, which is stronger pronounced at higher Al_2O_3 contents in the slag. Open remelting leads to a strong loss in silicon almost independent of the slag composition. In contrast, the content of aluminum in the ingots exhibits a clear correlation with the Al_2O_3 content in the slag, thereby the rise of the aluminum content is stronger pronounced for remelting under protective gas. For both trace elements, oxygen and sulfur, and open remelting, there is a general trend of highly increased oxygen contents and strongly reduced sulfur contents, almost independent of the slag composition. In contrast, there is a clear trend toward decreasing oxygen and sulfur values in the remelted ingot with falling Al_2O_3 contents in the slag. Using a practically Al_2O_3-free slag, sulfur can be removed almost completely, and the increase in oxygen is only weak.

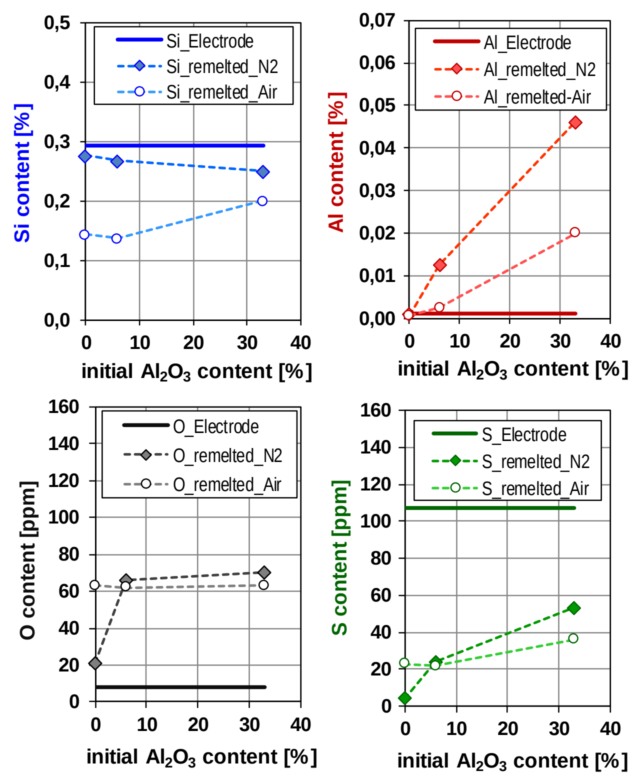

Figure 1. Changes of the chemical composition of the steel during remelting with different initial Al_2O_3 contents in the slag for open remelting and remelting under nitrogen.

3.2. Chemical Composition of the Slag After Remelting

Changes in the chemical composition of the slag, except for SiO_2, were rather minor (**Figure 2**). There was a slight increase in the SiO_2 content for the protective gas remelting, almost independent of the slag composition and a higher raise for open remelting. This goes hand in hand with high FeO contents for open remelting. During protective atmosphere remelting, a higher FeO content was only found in the slag with the highest alumina content. Changes in both oxides are clear indicators for chemical reactions occurring during the remelting process. The Al_2O_3 content remained almost unchanged. The only significant reduction of Al_2O_3 in the case of the high alumina slag and open remelting (trial A33) can be explained partially by a thinning effect of the additional SiO_2. Additional investigation on the slag composition of the slag cover on the ingots revealed that the SiO_2 content was about 2% lower than in the top slag.

3.3. Nonmetallic Inclusions

Subsequently, only the electrodes and those ingots that were remelted under protective atmosphere were selected for further investigations on NMI and simulations.

3.3.1. Content and Types of NMIs

NMIs were evaluated regarding their content (in area [%]), type (oxides oxisulfides, sulfides), size (equivalent cycle diameter [ECD]), and (chemical) composition. The content of all detected NMI is shown for comparison in **Figure 3**. The left diagram depicts this content, differentiated into larger NMI with an ECD > 5 μm (dark) and smaller ones with an ECD between 1 and 5 μm. As the continuous cast electrodes were supposed to be more inhomogeneous than the remelted ingots, two positions from the electrode (E-rim and E-core) were investigated. The results demonstrate the excellent quality of the electrode material. Remelting with a Al_2O_3-containing slags led to an significant increase in the NMI content, which was stronger pronounced at higher Al_2O_3 contents. Only with the practically Al_2O_3-free slag in trial A0-N an improvement, especially for larger NMI, could be achieved.

The chart on the right shows the proportional share of oxides, oxisulfides, and oxides in relation to the total content of NMI, indicating a strong increase in oxides and oxisulfides during remelting with Al_2O_3 containing slags. In reverse, pure sulfides largely disappear during remelting, almost independent of the slag composition. Furthermore, the content of oxides correlates well with the measured oxygen content in the steel. As almost all detected NMI were of the types oxides, sulfides, and their

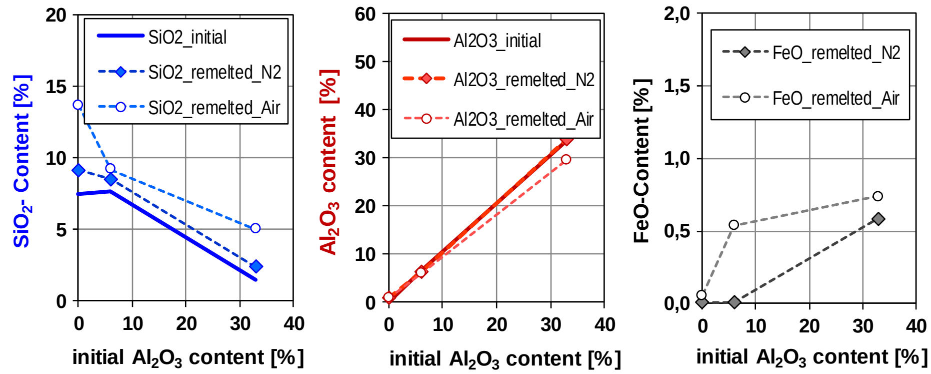

Figure 2. Changes of the chemical composition of the slag during remelting with different Al_2O_3 contents in the slag.

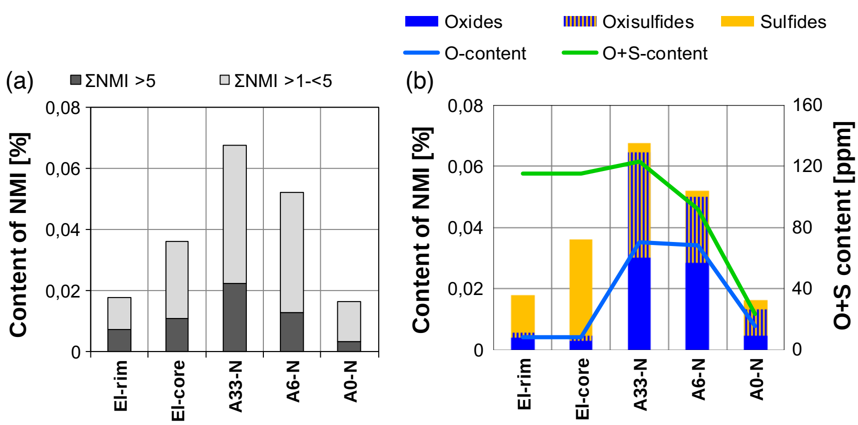

Figure 3. Content of NMIs in the electrode (two positions) and in the remelted ingots using different Al_2O_3 contents in the slag; a) differentiation by the size; b) differentiation by the NMI type in correlation with the oxygen and sulfur contents.

mixtures, there is also a good correlation between the total content of NMI and the summarized content of oxygen + sulfur for all remelted ingots. In contrast, for the electrode, the amount of oxygen + sulfur (where the same check analysis is used for both positions) is much higher than the detected content of NMI.

3.3.2. Chemical Composition of NMIs

The chemical composition of NMI is documented in the ternary system Al_2O_3–SiO_2–MgO in **Figure 4** and **5**, representing the main components of the vast majority of all detected oxides and the oxidic parts of the oxisulfides. The analyzed compositions were projected to 100% by keeping their measured shares of Al_2O_3, SiO_2, and MgO contents. White areas represent compositions without NMI. Blue areas correspond to compositions where only few NMI could be detected. Compositions with high numbers of inclusions are marked in red. Sulfides were not included in these figures and were always of MnS type.

Both positions of the electrode show a majority of high Al_2O_3–SiO_2-containing NMI with low amounts of MgO. In case of the center position, a clear mullit-type inclusion is dominating. In the outer position, additionally a mixed MgO–SiO_2 olivin type (≈forsterite) was found.

Remelting with the high (33%) alumina-containing slag leads to a complete change of the oxides to almost pure Al_2O_3 inclusions (Figure 5, top). A lower alumina contents in the remelting slag of 6% resulted in roughly spinel-type (MgO·Al_2O_3) inclusions, with a wider scatter of their, MgO/Al_2O_3 ratio (Figure 5, middle). Using the alumina-free slag 0 A changes the composition of the NMI toward dominantly MgO-containing inclusions, however, the results in Figure 5 (bottom) also show a wider scatter of mixed inclusions with various amounts of dominantly MgO and SiO_2 as well as some inclusions with a slightly increased Al_2O_3 content.

3.3.3. Simulation Results on the Formation of NMIs

The simulation on NMI formation in the electrode showed only very limited coherency with the measured results, therefore,

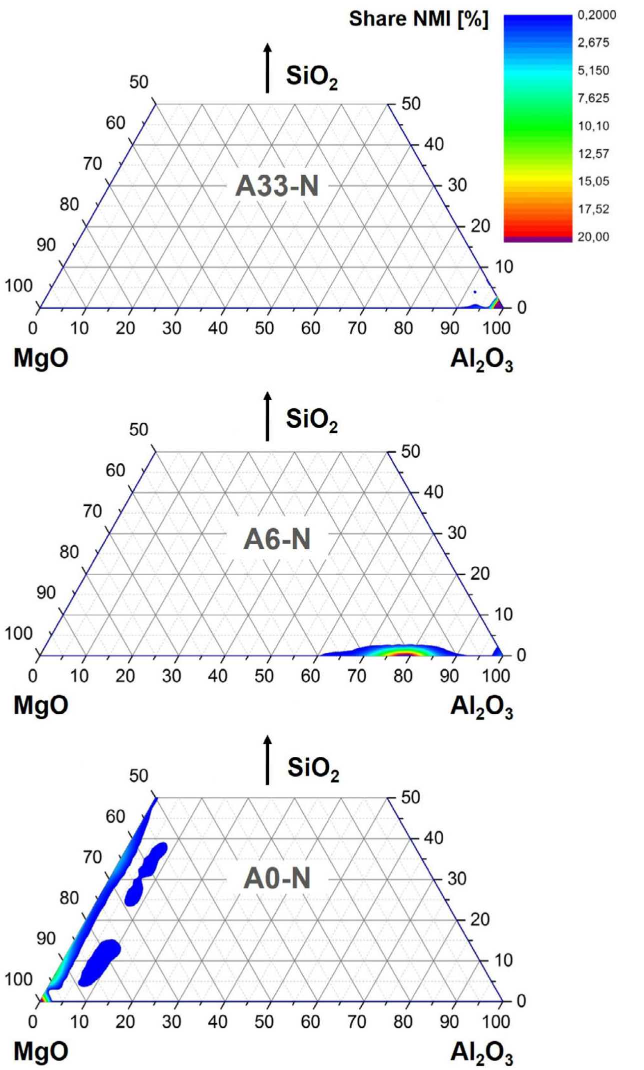

Figure 5. Chemical composition of NMI in the remelted ingots in the ternary system Al_2O_3–SiO_2–MgO; top: A33-N, middle: A6-N, and bottom: A0-N.

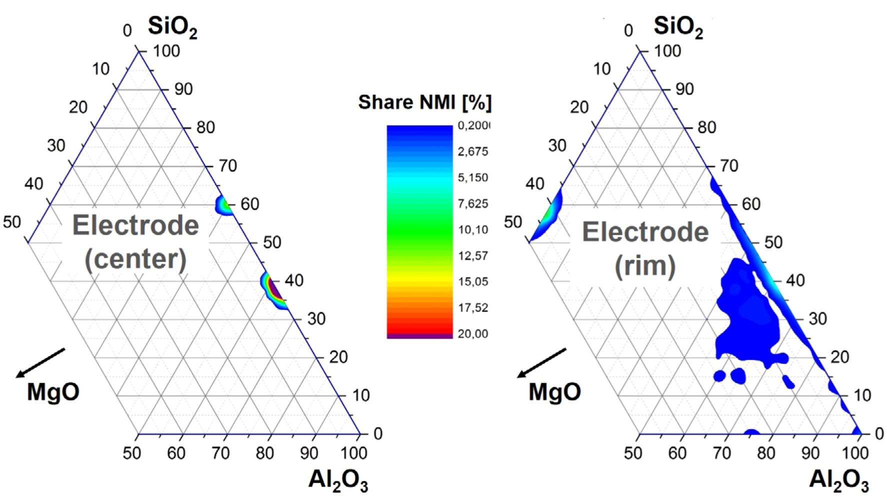

Figure 4. Chemical composition of NMI in the electrode in the ternary system Al_2O_3–SiO_2–MgO; left: center and right: rim.

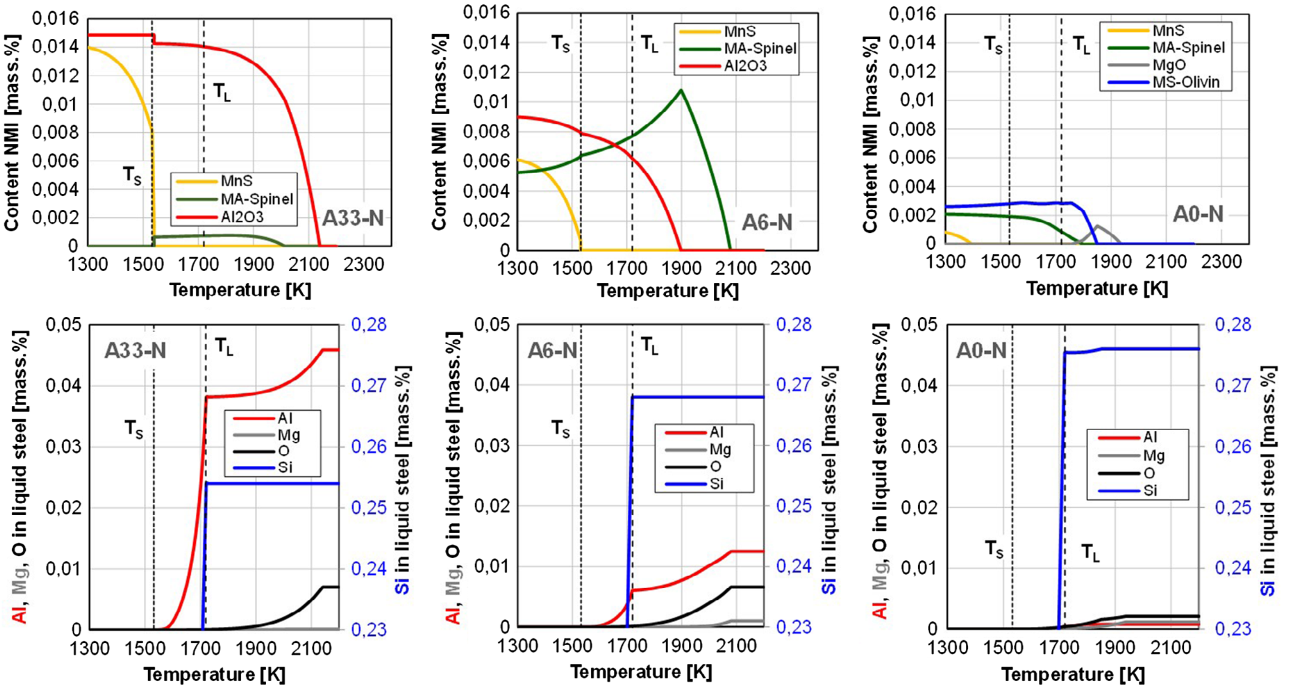

Figure 6. Formation of NMI during cooling and solidification after remelting calculated with "FactSage 7.3"; top: oxide and sulfide formation with falling temperature, bottom: changes of Al, Si, O, and Mg contents in the liquid steel with falling temperature; left: A33-N, middle: A6-N, and right: A0-N.

these results are not on display in the article. A reason for this divergence can be found in the solidification conditions during continuous casting and corresponding segregations, which cannot be described by simple equilibrium conditions.

The calculated results for the remelted ingots is shown in **Figure 6**. The scales are kept the same for all three ingots to allow best comparability. The slag with the highest alumina content of 33% (Figure 6, left), which lead to the highest aluminum and oxygen contents in the steel, results in the formation of large quantities of almost pure Al_2O_3 inclusions, starting about 400 °C above the liquidus temperature T_L (1720 K) of the steel. Below 2000 K, a small amount of MA-spinel is formed. The formation of manganese sulfides (MnS) starts with a rapid growth just above the solidus temperature of 1526 K and leads to an almost similar content as for the oxides. The lower chart shows clearly that the corresponding reduction of aluminum (459 ppm) und oxygen (70 ppm) in the liquid steel, while the silicon content remains unchanged. The contribution of magnesium (1 ppm) is very limited.

After remelting with the 6% Al_2O_3-containing slag (Figure 6, middle, A6-N), the reduced aluminum (125 ppm) and increased magnesium (10 ppm) contents in the steel react with the still high oxygen content (66 ppm) to form MA-spinel at about 2100 K. When all magnesium is consumed at about 1900 K, parts of the MA-spinel transforms into rising amounts of almost pure Al_2O_3 inclusions, ending with a mixture of these two types of oxides. Despite the significantly lower aluminum content, silicon does not participate in the formation of oxides. Due to a significantly lower sulfur content, the formation of MnS is much less than in trial A33-N, but the formation also starts at the solidus temperature of the steel.

The very low aluminum content (8 ppm) in the steel after remelting with alumina-free slag in combinations with the lower oxygen (21 ppm) and the high magnesium content (12 ppm) leads to completely different NMI formation (Figure 6, right). At first, pure MgO inclusions start to form above 1900 K, which in a second step, are completely transformed into MgO- and SiO_2-containing olivine-type inclusions. Finally, also a small amount of MA-spinel is formed. The involvement of silicon in the NMI formation is shown in a slight reduction of the silicon content of the liquid steel during NMI formation below 1850 K. As a consequence of the very low sulfur content of the MnS is only formed in very small quantities from solid solution.

4. Discussion

4.1. Chemical Reactions and Changes in the Composition of Steel and Slag

The reduction of the silicon content and the corresponding increase in aluminum in the steel after remelting with the 6% and 33% Al_2O_3-containing slag depends, in accordance with previous studies,[12,13,19–21,23,30,37] mainly on the chemical reaction according to Equation (1)

$$3[Si] + 2(Al_2O_3) \leftrightarrow 3(SiO_2) + 4[Al] \tag{1}$$

which describes the equilibrium between Si and Al in the steel and the content (activity) of SiO_2 and Al_2O_3 in the slag. During open remelting without protective atmosphere, scaling of iron to iron oxide at the electrode surface above the slag, according to

Equation (2), is the main source of oxygen uptake into the slag.[16,24]

$$O_2(g) + Fe(s) \leftrightarrow (FeO) \tag{2}$$

Consequently, an additional loss of silicon and increase in SiO_2 according to Equation (3) can be observed in trials A33, A6, and A0, which agrees well with statements in previous studies.[12,13,19,23]

$$[Si] + 2[O] \text{ or } 2(FeO) \leftrightarrow (SiO_2) + 2Fe \tag{3}$$

Based on Equation (1), these higher SiO_2 contents in the slag reduce the aluminum uptake in the steels. Furthermore, both oxides, SiO_2 and Al_2O_3 stay in equilibrium with the melt according to Equation (4) and (5)

$$[Si] + 2[O] \leftrightarrow (SiO_2) \tag{4}$$

$$2[Al] + 3[O] \leftrightarrow (Al_2O_3) \tag{5}$$

A decomposition of Al_2O_3 according to Equation (5) is the main reason for the simultaneous increasing aluminum and oxygen contents in the ingot after remelting with alumina-containing slags, especially when remelting is conducted under a protective atmosphere.

Furthermore, fluoride-containing ESR slags are not completely stable and changes in the composition through the volatilization according to e.g., Equation (6) are possible.[37,38]

$$3(CaF_2) + (Al_2O_3) \leftrightarrow 2\{AlF_3\} + 3(CaO) \tag{6}$$

However, this effect is most pronounced in high Al_2O_3 containing, low CaO, or CaO-free slag systems, and the reaction is gradually. A similar behavior could be found in $\geq$20% SiO_2-containing slags and a corresponding SiF_4 formation.[38] As such types of slag were not used in these experiments and probably also due to the significantly shorter process duration compared with some industrial processes, no significant volatilization losses could be found by mass balances between the initial amount of slag and the combined top skin and slag after remelting.

For a complete understanding of the results, however, desulfurization based on Equation (7) and (8), as described in previous studies,[12,23,24] has to be considered also. Thereby, the regeneration of the slag based on Equation (8) is only relevant for open remelting, leading to lower sulfur contents in the remelted steels when Al_2O_3-containing slags are used.

$$2[S] + 2(O^{2-}) \leftrightarrow 2[O] + 2(S^{2-}) \tag{7}$$

$$2(S^{2-}) + 3\{O_2\} \leftrightarrow 2\{SO_2\} + 2(O^{2-}) \tag{8}$$

For a basicity (CaO/SiO_2) lower than 1.5, a significantly lower desulfurization can be expected.[39] Higher Al_2O_3 contents reduce the basicity as well, which provides an additional explanation for the limited desulfurization of both trials with 33% Al_2O_3 content in the slag. The reduction of sulfur content in all remelting trials, is in good agreements with the expected process behavior according to the description in previous studies.[12,24,39]

The exchange reaction between oxygen and sulfur from Equation (7) is, in addition to scaling at open remelting (Equation (2) and (3)) and alumina decomposition (Equation (5)), the third main source of oxygen pick up to the steel. This is most relevant for trial A0-N, where the protective gas prevents scaling and Al_2O_3 decomposition is limited by an almost alumina-free slag. Under these conditions, desulfurization based on Equation (7) is very effective. Most of the oxygen that is correspondingly transferred to the melt is subsequently removed by silicon and, to a much lower extent, also aluminum according to Equation (4) and (5), resulting in low sulfur and oxygen contents in the steel at only limited losses of silicon and aluminum.

4.2. Nonmetallic Inclusions

In agreement with findings in previous studies,[29,30,38,40] the remelted ingots show a significant reduction in sulfides and a good correlation of the NMI content and their specific types (oxides, oxislufides, and sulfides) with the corresponding contents of oxygen and sulfur in the steel. As oxides often act as nucleus for the sulfide formation,[16,19] the rising content of oxides after remelting with alumina-containing slag also leads to a higher content of mixed type oxisulfides. For the electrode, there is also a good correlation of the oxygen content and the oxides at both positions but, especially at the rim, a significant discrepancy of the sulfur content with the sulfides. A potential reason for this discrepancy could be strong segregations of especially larger sulfides in combination with different sample volumes analyzed by chemical analysis and SEM. The NMI of the type mullite, which is dominating in the electrode, is typical for roller bearing steels.[33] Al_2O_3 and MA-spinel-type NMI are often found in steels after remelting with alumina- and MgO-containing slags[20,23,24,27–30,38] but, according to previous studies,[3,11,33] Al_2O_3-type NMI have significant negative effects on fatigue properties. Only with the alumina-free slag, the oxygen and the aluminum contents in the liquid bath can be kept low enough to avoid Al_2O_3. The formation of chemically completely different types of NMI in the remelted ingots compared with the electrode confirms, in agreement with previous studies,[16,18,19,23,30,31] that they are newly formed during solidification, and are no survivors from the electrode, as described in the studies by Sjöqvist Persson et al.[25,26] While Al_2O_3-containing slags are used widely and successfully in industrial applications for several decades to remove large NMI, especially sulfides, Al_2O_3-free slags systems have gained more interest in recent years[38,41] and offer the additional option to change the type of oxide inclusion.

Thermodynamic calculations by Factsage showed a good general agreement, both in composition and content, with those NMI detected with SEM–EDS for all three remelted ingots. However, the forming sequence from high temperature has to be considered. In case of trial A33-N with high aluminum and oxygen contents, alumina inclusions are primarily formed. These are also the dominant type of inclusions detected in the material. Later on a small amount of MA-spinel inclusions are predicted. Such specific type of inclusions was not detected, but there is a small population of Al_2O_3-rich NMI with a higher MgO content, which indicates that some MgO-containing inclusions are formed. This is in good agreement with experimental and simulation results in the study by Shi and Park,[30] where also mixtures of Al_2O_3 and MA-spinel inclusions were detected and predicted after remelting with a high alumina-containing slag.

In case of remelting with the 6% alumina-containing slag (trial A6-N), having a much lower aluminum, a severely higher magnesium, and a similar oxygen content, the formation of NMI starts with MA-spinel which is later on partially transferred to and complemented with alumina inclusions. This corresponds well with the wide-stretched area ranging from about 60% to 90% Al_2O_3 composition and indicate, that mixed types inclusions and not two separate populations of inclusions were formed.

The low aluminum and oxygen contents combined with high magnesium concentration in the liquid steel of trial A0-N lead first to the formation of pure MgO inclusions. These inclusions should be transformed completely to MgO–SiO_2-type olivine (forsterite) at lower temperature, but can still be found in a significant share in the steel. The wide region of mixed MgO–SiO_2 inclusions with two focal areas, one at very high MgO contents (85–95% MgO) and one with lower MgO contents (60–70% MgO), demonstrate that two different origins, a transformation of MgO and separate formation of forsterite, is likely. The predicted formation of MA-spinel could not be confirmed by these measurements, but there are some inclusions with 5–10% Al_2O_3, which can be understood as conglomerates of the former two focal areas of MgO–SiO_2 inclusions with low amounts of MA-spinel.

5. Conclusions

The Al_2O_3 content of the remelting slag has a strong effect on the chemical composition of the steel after remelting. By reducing the alumina content, the aluminum and the oxygen contents in the steel are kept at low levels. The sulfur content is most strongly reduced, and the silicon content is lowered only slightly.

A protective atmosphere during remelting prevents the oxidation of the electrode and leads to higher silicon and aluminum contents in the steel. An advantage of the protective atmosphere on the oxygen and sulfur contents could only be found for the Al_2O_3-free slag.

The reduction of Al_2O_3 in the remelting slag results in lower amounts of NMIs (oxides, oxisulfides), which correlates well with the lower oxygen and sulfur contents.

The Al_2O_3 content of the remelting slag has also a significant effect on the composition of the NMI. With ≈33% alumina in the slag almost pure Al_2O_3 type inclusions are formed, ≈6% alumina in the slag lead to MA-spinel-type inclusions and remelting with alumina-free slags produce dominantly high MgO and MgO–SiO_2 (forsterite)-type inclusions.

Sulfides (essentially MnS type) were removed by all remelting trials, but the effect was dominant using the alumina-free slag.

Starting from the chemical composition after remelting, the formation of NMI can be well described by thermodynamic simulation with "FactSage 7.3" in "Eqilib" mode.

Acknowledgements

The authors gratefully acknowledge the funding support of K1-MET GmbH, metallurgical competence center. The research programme of the K1-MET competence center was supported by Competence Center for Excellent Technologies (COMET), the Austrian programme for competence centers. COMET is funded by the Federal Ministry for Climate Action, Environment, Energy, Mobility, Innovation and Technology, the Federal Ministry for Digital and Economic Affairs, the Federal States of Upper Austria (grant number 869295), Tyrol and Styria as well as the Styrian Business Promotion Agency (SFG). In addition to the public funding from COMET, this research project was partially financed by scientific partners and the industrial partner voestalpine Stahl Donawitz GmbH.

Conflict of Interest

The authors declare no conflict of interest.

Keywords

Al_2O_3 contents, chemical reactions, electroslag remelting, nonmetallic inclusions, protective gases, simulations

Received: April 30, 2020
Revised: June 19, 2020
Published online: July 26, 2020

[1] M. Oezel, T. Janitzky, P. Beiss, C. Broeckmann, *Wear* **2019**, *430–431*, 272.
[2] A. L. Vasconcellos da Costa e Silva, *J. Mater. Res. Technol.* **2019**, *8*, 2408.
[3] H. Fu, J. J. Rydel, A. M. Gola, F. Yu, K. Geng, C. Lau, H. Luo, P. E. J. Rivera-Diaz-del-Castillo, *Int. J. Fatigue* **2019**, *129*, 104899.
[4] K. Furumura, Y. Murakami, T. Abe, *Motion Control* **1996**, *1*, 30.
[5] P. F. F. Walker, *Mater. Sci. Technol.* **2014**, *30*, 385.
[6] M. W. J. Lewis, B. Tomkins, *Proc. Inst. Mech. Eng. Part J* **2012**, *226*, 389.
[7] G. Donzella, M. Faccoli, A. Mazzù, C. Petrogalli, H. Desimone, *Eng. Fract. Mech.* **2011**, *78*, 2761.
[8] T. B. Lund, *J. ASTM Int.* **2010**, *7*, 81.
[9] F. J. Ebert, *Chin. J. Aeronaut.* **2019**, *23*, 123.
[10] K. Hashimoto, T. Fujimatsu, N. Tsunekage, K. Hiraoka, K. Kida, E. Costa Santos, *Mater. Des.* **2011**, *32*, 4980.
[11] K. Hashimoto, T. Fujimatsu, N. Tsunekage, K. Hiraoka, K. Kida, E. Costa Santos, *Mater. Des.* **2011**, *32*, 1605.
[12] W. Holzgruber, E. Plöckinger, *Stahl Eisen* **1968**, *88*, 638.
[13] W. Holzgruber, E. Plöckinger, *Berg-Huettenmaenn. Monatsh.* **1968**, *113*, 83.
[14] E. Plöckinger, *J. Iron Steel Inst.* **1973**, *211*, 533.
[15] A. Mitchell, *J. Mater. Sci. Eng. A* **2005**, *413–414*, 10.
[16] C.-B. Shi, X.-C. Chen, H.-J. Guo, Z.-J. Zhu, H. Ren, *Steel Res. Int.* **2012**, *83*, 472.
[17] C. K. Mills, B. J. Keene, *Int. Met. Rev.* **1981**, *1*, 21.
[18] A. Mitchell, *Ironmaking Steelmaking* **1974**, *1*, 172.
[19] A. Mitchell, F.-R. Carmona, C.-H. Wei, *Ironmak. Steelmak.* **1982**, *9*, 37.
[20] M. Allibert, J. F. Wadier, A. Mitchell, *Ironmak. Steelmak.* **1978**, *5*, 211.
[21] S. Radwitz, H. Scholz, B. Friedrich, H. Franz, in *LMPC 2015, Proc. Int. Symp. Liq. Met. Process. Cast.*, (Eds: A. Kharicha, M. Ward, H. Holzgruber, M. Wu), ASMET, Leoben **2015**, p. 1.
[22] H. Miska, M. Wahlster, *Arch. Eisenhuettenwes.* **1973**, *44*, 19.

[23] R. S. E. Schneider, M. Molnar, S. Gelder, G. Reiter, C. Martinez, *Steel Res. Int.*, **2018**, *89*, 1800161.
[24] Y.-W. Dong, Z.-H. Jiang, Y.-L. Cao, A. Yu, D. Hou, *Metall. Mater. Trans. B* **2014**, *45*, 1315.
[25] E. Sjöqvist Persson, A. Mitchell, in *LMPC 2017, Proc. Int. Symp. Liq. Met. Process. Cast.*, (Eds: M. J. M. Krane, R. M. Ward, S. Rudoler, A. J. Elliott, A. Patel), TSM, Philadelphia **2017**, p. 373.
[26] E. Sjöqvist Persson, A. Karasev, P. Jönsson, in *LMPC 2017, Proc. Int. Symp. Liq. Met. Process. Cast.*, (Eds: M. J. M. Krane, R. M. Ward, S. Rudoler, A. J. Elliott, A. Patel), TMS, Philadelphia **2017**, p. 353.
[27] G. Reiter, W. Schuetzenhoefer, A. Tazreiter, C. Martinez, P. Wuerzinger, C. Loecker, in *LMPC 2013, Proc. Int. Symp. Liq. Met. Process. Cast.*, (Eds: M. J. M. Krane, A. Jardy, R. L. Williamson, J. J. Beaman), TMS, Austin, **2013**, p. 213.
[28] J.-H. Liu, G.-X. Wang, Y.-P. Bao, Y. Yang, W. Yao, X.-N. Cui, *J. Iron Steel Res. Int.* **2012**, *19*, 1.
[29] R. Schneider, C. Schüller, P. Würzinger, G. Reiter, C. Martinez, *Berg- Huettenmaenn. Monatsh.* **2015**, *160*, 117.
[30] C. Shi, J. H. Park, *Metall. Mater. Trans. B* **2019**, *50B*, 1139.
[31] Z. Li, J. Zhang, Y. Li, C. Wang, *J. Iron Steel Res. Int.* **1998**, *5*, 34.
[32] A. Randak, A. Stanz, W. Verderber, *Stahl Eisen* **1972**, *92*, 981.
[33] G. Klösch, K. Huemer, A. Sormann, G. Frank, *Berg Hüttenmänn. Monatsh.* **2009**, *154*, 27.
[34] a) R. Schneider, M. Molnar, G. Klösch, C. Schüller, in *LMPC 2019, Proc. Liq. Met. Process. Cast. Conf. 2019*, (Eds: A. Jardy, A. Mitchell, R. M. Ward), TMS, Birmingham, UK **2019**, p. 175; b) R. Schneider, M. Molnar, G. Klösch, C. Schüller, *Metall. Mater. Trans. B* **2020**, https://doi.org/10.1007/s11663-020-01896-8.
[35] R. Schneider, A. Paar, P. Zeller, G. Reiter, W. Schützenhöfer, P. Würzinger, *Berg- Huettenmaenn. Monatsh.* **2011**, *156*, 112.
[36] R. Werl, G. Klösch, W. Winkler, A. Pissenberger, M. W. Egger, S. Aigner, J. Pühringer, S. Michelic, C. Bernhard, W. Schützenhöfer, R. Schneider, C. Schüller, *Berg Hüttenmaenn. Monatsh.* **2012**, *157*, 194.
[37] A. Mitchell, *Can. Metall. Q.* **1981**, *20*, 101.
[38] Y. Liu, Z. Zhang, G. Li, Y. Wu, X. Wang, B. Li, *Metal. Res. Technol.*, **2019**, *116*, 1.
[39] H. Miska, M. Wahlster, *Arch. Eisenhuettenwes.* **1973**, *44*, 81.
[40] R. Schneider, M. Mülleder, P. Zeller, P. Würzinger, G. Reiter, S. Paul, *Berg- Huettenmaenn. Monatsh.* **2016**, *161*, 20.
[41] J. Korp, R. Schneider, P. Presoly, W. Krieger, *Berg- Huettenmaenn. Monatsh.* **2008**, *153*, 175.